Journal of Experimental Botany, Vol. 73, No. 12 pp. 4250–4265, 2022
https://doi.org/10.1093/jxb/erac145 Advance Access Publication 6 April 2022

RESEARCH PAPER

Effects of high temperature and nitrogen availability on the growth and composition of the marine diatom *Chaetoceros pseudocurvisetus*

Lana Flanjak[1,*], Ivna Vrana[2], Ana Cvitešić Kušan[2], Jelena Godrijan[2], Tihana Novak[2], Abra Penezić[2] and Blaženka Gašparović[2,*]

[1] Department of Chemistry and Bioscience, Aalborg University, Fredrik Bajers Vej 7H, 9220 Aalborg, Denmark
[2] Laboratory for Marine and Atmospheric Biogeochemistry, Ruđer Bošković Institute, Bijenička cesta 54, 10000 Zagreb, Croatia

* Correspondence: lanafl@bio.aau.dk or gaspar@irb.hr

Received 18 November 2021; Editorial decision 30 March 2022; Accepted 4 April 2022

Editor: Christine Foyer, University of Birmingham, UK

Abstract

The assimilation of inorganic nutrients by phytoplankton strongly depends on environmental conditions such as the availability of nitrogen and temperature, especially warming. The acclimation or adaptation of different species to such changes remains poorly understood. Here, we used a multimethod approach to study the viability and physiological and biochemical responses of the marine diatom *Chaetoceros pseudocurvisetus* to different temperatures (15, 25, and 30 °C) and different N:P ratios. Nitrogen limitation had a greater effect than high temperature on cell growth and reproduction, leading to a marked elongation of setae, decreased phosphorus assimilation, increased lipid accumulation, and decreased protein synthesis. The elongation of setae observed under these conditions may serve to increase the surface area available for the uptake of inorganic and/or organic nitrogen. In contrast, high temperatures (30 °C) had a stronger effect than nitrogen deficiency on cell death, nitrogen assimilation, chlorophyll *a* accumulation, the cessation of setae formation, and cell lipid remodelling. Significant changes in thylakoid lipids were observed in cells maintained at 30 °C, with increased levels of digalactosyldiacylglycerol and sulfoquinovosyldiacylglycerol. These changes may be explained by the role of galactolipids in thylakoid membrane stabilization during heat stress.

Keywords: Biochemical response, *Chaetoceros pseudocurvisetus*, diatom, global warming, lipid remodelling, nitrogen stress, physiological response.

Introduction

It is unequivocal that human influence has warmed the atmosphere, oceans, and land (IPCC, 2021). Warming of the global ocean, in terms of both the surface temperature and the heat content, has significant impacts on sea level rise, oxygen concentration, acidification, and nutrient cycling, as well as primary production and carbon (C) sinks (IPCC, 2021). Global sea surface temperature increased by 0.88 °C between 1850–1900 and 2011–2020, with most of this warming mainly due

Abbreviations: C, carbon; Chl *a*, chlorophyll *a*; cell C:Chl *a*, cellular carbon-to-chlorophyll *a* ratio; CL, Cellular lipids; DGDG, digalactosyldiacylglycerol; DIN, dissolved inorganic nitrogen; DOC, dissolved organic carbon; GL, glycolipids, MGDG, monogalactosyldiacylglycerol; MSGR, maximum specific growth rate; N, nitrogen; N+, N-excess; N±, N-optimal; N–, N-limiting; P, phosphorus; PC, phosphatidylcholines; PE, phosphatidylethanolamines; PG, phosphatidylglycerols; PL, phospholipids; POC, particulate organic carbon; SE, steryl esters; PSII, Photosystem II; ST, sterols; SQDG, sulfoquinovosyldiacylglycerol; TG, triacylglycerols; TN, total cellular nitrogen.

to warming since 2003–2012, and the increase is projected to continue rapidly due to human activities (IPCC, 2021). However, the spatiotemporal trends of warming and the resulting changes differ significantly between different oceanic regions. The Mediterranean Sea is considered to be one of the regions most affected by climate change (Kim *et al.*, 2019). The average temperature in the Mediterranean Sea is 0.4 °C higher than the global average, with even more extreme seasonal variations (Nykjaer, 2009). The increased stratification of the seawater column caused by warming reduces the vertical nutrient supply from the deeper layers (oligotrophication of the surface layer), which has a direct negative impact on primary production. As a result, a decrease in chlorophyll *a* (Chl *a*) concentration has been observed in the western Mediterranean Sea since the 2000s, which is strongly correlated with the increase in sea surface temperature (Kim *et al.*, 2019). The increasing oligotrophication of the northern Adriatic Sea is explained by the reduced inflow of freshwater associated with the shortening of the snow cover period in the Italian Alps (Gašparović, 2012).

In contrast, coastal waters such as the Baltic Sea are exposed to anthropogenic nutrient inputs (Gustafsson *et al.*, 2012), which extend and accelerate the effects of eutrophication (Smil, 2004). Projections are dire and suggest that the problem will be exacerbated by nutrient fluctuations in upwelling areas, extreme rainfall followed by runoff, and increased oxygen-depleted dead zones (Bindoff *et al.*, 2019). These physico-chemical changes will subsequently affect the diversity, abundance, and structure of marine communities.

Phytoplankton play an important role in the C cycle by photosynthetically fixing ~45 billion tons of C per year. In addition, phytoplankton supply organic matter to higher trophic levels in the food web (Falkowski and Woodhead, 1992) and sink towards the ocean floor (biological C pump), also playing an important role in regulating global CO_2 on a longer time scale (Falkowski, 1997). In the era of global climate change, phytoplankton are adapting in terms of their abundance, cellular composition of biomolecules (lipids, sugars, and proteins), biochemical and morphological properties, surface features, and physiological activity of the cell (Novosel *et al.*, 2021). Consequently, these changes are expected to influence the quantity and quality of organic matter exported to the deep ocean (a long-term sink for CO_2) as well as to higher trophic levels.

Diatoms are one of the most important groups of phytoplankton (Malviya *et al.*, 2016), contributing to 25–30% of oceanic primary production (Uitz *et al.*, 2010). When conditions are optimal for their growth, diatoms tend to dominate phytoplankton communities (Bopp *et al.*, 2005). They are very efficient at transporting C to the ocean interior (Passow and Carlson, 2012), particularly due to their tendency to form large, rapidly sinking aggregates (Smetacek, 1985). As a result of surface warming and the associated increase in vertical stratification, unfavourable oligotrophic conditions for diatoms are occurring on a larger scale in the surface ocean (Bopp *et al.*, 2005). These stressors not only alter the relative abundance and species structure of diatom communities, but also affect these microalgae on the physiological level. Studies have reported various cellular responses to nutrient limitation and temperature increases. Of particular interest are the effects of nitrogen (N) depletion, as productivity in most of the ocean (~75%) is limited by the availability of inorganic N (Bristow *et al.*, 2017). A variety of adaptations to N stress have been observed in diatoms, such as reorganization of the cell proteome, disruption of the photosynthetic apparatus, and reduced growth, cell size, and net primary production (Berges *et al.*, 1996; Jiang *et al.*, 2012; Longworth *et al.*, 2016; Ko *et al.*, 2020). At the same time, temperature increases have led to higher growth rates, a decrease in cell size and cellular C-to-Chl *a* ratio (cell C:Chl *a*), and C partitioning between major biochemicals (Anning *et al.*, 2001; de Castro Araújo and Garcia, 2005; Liang *et al.*, 2019). Both N depletion and sea surface warming have been found to trigger lipid remodelling in marine diatoms (Novak *et al.*, 2019). Lipids are essential biomolecules that play an important role in supporting living cells by forming membranes, storage reserves, and signalling pathways. Characterization of marine lipids at the molecular level enables their use as biogeochemical markers for identifying various sources and processes of organic matter in the ocean (Parrish, 1988; Gašparović *et al.*, 2013).

Here, we investigated the influence of the combination of different temperatures (15 °C as optimal and 25 °C and 30 °C as temperature stress) and varying inorganic N availability, mimicking optimal, eutrophic, and oligotrophic conditions, on the cellular response of the model marine diatom *Chaetoceros pseudocurvisetus*. *Chaetoceros* is the largest and most diverse diatom genus found in wide range of oceanic regions (Malviya *et al.*, 2016), and has been consistently present in (Bosak *et al.*, 2016) and considerably contributing to the phytoplankton community in the northern Adriatic Sea (Novak *et al.*, 2018, 2019). Experiments were conducted under non-axenic conditions (an intrinsic feature of seas and oceans) to allow circulation of nutrients by heterotrophs, which has been shown to benefit autotrophs (Christie-Oleza *et al.*, 2017). The two main questions we were interested in were (i) which of the stressors studied has a greater negative impact on specific physiological and biochemical processes in the cell, and (ii) whether the negative impact increases when the two stressors act synergistically. To answer these questions, we performed experiments with a monoclonal culture of *C. pseudocurvisetus* and performed nine cultivation treatments, including the combination of three temperatures with N-excess, optimal N:P ratio, and N-limiting conditions.

Materials and methods

Microalgae cultures

The chosen experimental organism, the diatom *Chaetoceros pseudocurvisetus* Mangin 1910, was isolated from the northern Adriatic Sea and was shown

to be very amenable to experimental manipulation (Novak et al., 2018, 2019). A monoclonal culture was established from a *C. pseudocurvisetus* colony isolated from a sample collected in October 2014 in the northern Adriatic Sea. The culture was maintained in F/2 medium (Guillard, 1975) at 15 °C, 4500 lux, and a 12 h light/12 h dark photoperiod.

Cultivation setup

Chaetoceros pseudocurvisetus was grown in triplicate in sterile Erlenmeyer flasks of 2000 ml capacity, with a culture volume of 1000 ml covered with a Petri dish, at three different temperatures (15, 25, and 30 °C). The Erlenmeyer flasks were cleaned with chromosulfuric acid and autoclaved before use for cell cultivation. The growth media were prepared according to Guillard (1975), adjusting the N and P concentrations and ratios. The experiment was designed to grow diatoms under the following conditions: N-excess (N+), N:P=50:1; optimal (N±), N:P=16:1; and N-limiting (N–), N:P=2:1. The optimal condition was chosen based on empirical data on the amount of N and P consumed at 15 °C (Novak *et al.*, 2019). The dissolved inorganic N (DIN; NO_3^-+NO_2^-+NH_4^+) concentrations of the N+, N±, and N– medium were 750.65 ± 2.62, 240.65 ± 2.62, and 30.65 ± 2.62 µmol l^{-1}, respectively. The PO_4^{3-} concentration was 15.05 µmol l^{-1} in all media. Control conditions were as follows: 15 °C, 240.65 ± 2.62 µmol l^{-1} DIN, and 15.05 µmol l^{-1} PO_4^{3-}.

The natural seawater used for the preparation of the media was obtained from a depth of 20 m in the Stončica Bay on the coast of the island of Vis in the middle Adriatic Sea (43° 3′ 58.08″ N, 16° 14′ 33.22″ E). Before further treatments, the collected seawater was stored in the dark for several months to ensure minimal organic matter content. Aged water was filtered through 0.7 µm Whatman GF/F filters and subjected to 24 h UV irradiation to remove any remaining bacteria and organic matter. The dissolved organic C (DOC) concentration after UV treatment was 0.30 ± 0.04 mg l^{-1}.

The experiment was started with 10^5 cells l^{-1} in a thermostatic chamber (Inkolab, Croatia), a 12 h light/12 h dark cycle under illumination of ~4500 lux, with a white LED light source. The inoculum was taken from preconditioned cultures in the exponential growth phase. Prior to inoculation, cells were maintained in F/2 replete media in 250 ml VWR® Tissue Culture Flasks (VWR, Radnor, PA, USA) under the respective temperature of the experiment. All cultures were grown in the same growth chamber to prevent the possible influence of factors other than those being tested. Cultures were shaken manually twice a day. Growth was ended at the beginning of the stationary growth phase. However, the majority of data suggest that the growth of the optimal culture (N±) at 25 °C was terminated too early (having erroneously assumed the onset of the stationary phase).

C. pseudocurvisetus growth, cellular carbon, and morphology

To determine *C. pseudocurvisetus* growth rates in each of the conditions, subsamples of 2 ml were taken daily and cells were counted using Sedgewick Rafter Counting Chambers under an Olympus BX51-P polarizing microscope. The maximum specific growth rate was calculated from the slope of the linear portion of the exponential (logarithmic phase) part of the growth curve as follows:

$$\mu = \frac{\ln(N_t) - \ln(N_0)}{t}$$

where N_t is the cell concentration (cell l^{-1}) at time t, N_0 is the cell concentration at the beginning of the logarithmic growth phase, and t indicates the duration of the logarithmic growth phase.

Additional subsamples (2 ml) from the early stationary growth phase were collected for cellular C calculation and visualization of morphological changes, and stored in formaldehyde solution until processing within 2 weeks. Images were acquired using a Zeiss Axio Observer 7 inverted microscope. Zen 3.3 software was used for image analysis. Cell width and length were measured and, assuming that the cells have a cylindrical shape, the cell volume was calculated. The C content of the cells was determined according to the calculations of Menden-Deuer and Lessard (2000). The share of cellular C in particulate organic C (POC) was calculated as:

$$\text{Cell C in POC}\,(\%) = \frac{(\text{Cell C} \times 100) \times \text{cell abundance}}{\text{POC}}$$

For morphological analysis, the length of at least 800 setae was measured.

Chl *a* analysis

For Chl *a* analysis, 50 ml of the culture medium was filtered through pre-combusted (450 °C for 5 h) Whatman GF/F filters (0.7 µm) and the filters were stored at –20 °C until extraction. Filters were immersed in 100% ethanol, incubated at 60 °C for 1 h, extracted at 4 °C in the dark for 24 h, and filtered (according to ISO 10260:1992; International Organization for Standardization, 1992). Chl *a* concentration was determined spectrophotometrically using a Shimadzu UV-1280 spectrophotometer (Shimadzu, Japan).

The Chl *a* concentration was calculated as follows:

$$\text{Chl } a = 29.6 \times (\text{A1} - \text{A2}) \times \frac{V_e}{V \times d}$$

where A1=(A665–AB665)–(A750–AB750) is the absorbance before acidification at 665 nm, corrected by turbidity adjustment at 750 nm (A is for sample and AB is for blank); A2=(AK665–ABK665)–(AK750–ABK750) is the absorbance after acidification at 665 nm, corrected by turbidity adjustment at 750 nm (AK is for sample and ABK is for blank); V_e is the volume of the extract; V is the total volume of the filtered sample; d is the path length of the cuvette; and 29.6 is a constant calculated from the maximum acid ratio (1.7) and the specific absorption coefficient of Chl *a* in ethanol (82 g l^{-1} cm) (International Organization for Standardization, 1992).

Nutrient analysis

Subsamples for nutrient analysis were filtered through 0.7 µm Whatman GF/F filters and filtrates (180 ml) were collected and stored at –20 °C until analysis. Spectrophotometric determination of the concentration of NO_3^-, NO_2^-, NH_4^+, and PO_4^{3-} was performed using a Shimadzu UV-1280 spectrophotometer (Shimadzu, Japan) with 1 cm quartz cuvettes (Strickland and Parsons, 1968).

Particulate and dissolved organic carbon analysis

For POC analysis, 40 ml of the culture medium corresponding to the early stationary phase was filtered through 0.7 µm Whatman GF/F filters, which were pre-combusted at 450 °C for 5 h. The filters were stored at –60 °C until analysis. Measurements were performed using the high-temperature catalytic oxidation method using the solid sample module SSM-5000A connected to a TOC-V_{CPH} C analyser (Shimadzu, Japan), calibrated with glucose (Sugimura and Suzuki, 1988). POC concentrations were corrected using blank filter measurements. The average filter blank value with the instrument blank corresponded to 0.005 mg C l^{-1}. The reproducibility for the glucose standard was 2%.

For DOC analysis, the dissolved fraction remaining after filtration of the culture medium for lipid analysis was collected in triplicate in 22 ml

glass vials combusted at 450 °C for 4 h. Samples were preserved with 100 µl mercury chloride (10 mg l^{-1}) and stored in the dark at 4 °C until analysis. A C analyser (model TOC-V_{CPH}, Shimadzu, Japan) with a Pt/Si catalyst and a non-dispersive infrared detector for CO_2 measurements was used for DOC measurements and calibrated with potassium hydrogen phthalate. Concentrations were calculated as an average of the three replicates. The average instrument and ultrapure water blank corresponded to 30 µg C l^{-1} with high reproducibility (1.5%).

Lipid analysis

For lipid analysis, subsamples (100 ml) were filtered through 0.7 µm combusted (450 °C for 5 h) Whatman GF/F filters, which were then stored at −60 °C until extraction. Particulate lipids were extracted along with added internal standard (stearic acid methyl ester), following a modified procedure (Bligh and Dyer, 1959). Internal standard was added to each sample to estimate the recoveries in the subsequent steps of sample analysis. Extracts were evaporated to dryness under N flow and dissolved in 20–40 µl of dichloromethane (Merck, USA) before analysis. Separation and identification of lipid classes was performed by Iatroscan thin-layer chromatography coupled with flame-ionization detection (Iatroscan MK-VI, Iatron, Japan). The Iatroscan was operated at a hydrogen flow rate of 160 ml min^{-1} and an air flow of 2000 ml min^{-1}. The analysed lipid classes, separated on Chromarods III, comprised hydrocarbons, steryl esters (SE), fatty acid methyl esters, fatty ketones, triacylglycerols (TG), free fatty acids, fatty alcohols, 1,3-diacylglycerols, sterols (ST), 1,2-diacylglycerols, pigments, monoacylglycerols, glycolipids (GL) including monogalactosyl-, digalactosyl-, and sulfoquinovosyldiacylglycerols (MGDG, DGDG, and SQDG, respectively), and phospholipids (PL) including phosphatidylglycerols (PG), phosphatidylethanolamines (PE), and phosphatidylcholines (PC). The total lipid concentration was calculated as the sum of all detected lipid classes. The detailed procedure is described in Gašparović *et al.* (2015, 2017).

Protein analysis

Samples for protein determination were prepared by a modified Lowry method (Lowry *et al.*, 1951; Price, 1965). Lowry reagents A, B, C, and D were prepared according to Slocombe *et al.* (2013). Subsamples (10 ml) were filtered through 0.7 µm Whatman GF/F filters, which were precombusted at 450 °C for 5 h. The filters were stored at −60 °C until extraction. Prior to extraction, the filters were cut into small pieces and 3 ml of Lowry reagent D was added, mixed, and incubated in centrifuge tubes (15 ml) with screw caps in a thermoblock at 55 °C for 1 h. After incubation, samples were cooled to room temperature and centrifuged at 4300 *g* for 35 min (Rotofix 32A, Germany). The protein extract (200 µl) was placed in a 96-well flat-bottomed microplate (NUNC, Roskilde, Denmark) and shaken well. Then, 20 µl of diluted Folin-Ciocalteu phenol reagent (2 N Folin-Ciocalteu phenol reagent:ultra-pure water 1:1) was added, shaken well, and after 30 min at room temperature in the dark, the plate was read at 600 nm (Tecan Infinite M200, Austria). The estimated protein content was determined by comparison with a standard protein bovine serum albumin calibration curve.

Data analysis

Data in this study are reported as mean ± SD values from triplicate analyses. ANOVA and Tukey post-hoc test, Pearson's correlation coefficient, and Shapiro–Wilk test were performed in SPSS statistical software, and significance was accepted at $P<0.05$ (unless stated otherwise). Two-way ANOVA followed by Tukey post-hoc test were performed in Origin 7 software. Curve fitting was performed in OriginPro 9 assuming sigmoidal growth of batch cultures.

Results

Effect of warming and N availability on C. pseudocurvisetus *physiology and morphology*

Cultures of *C. pseudocurvisetus* were grown at three different temperatures (15, 25, and 30 °C) and under three different nutrient conditions (N+, N±, and N–) to investigate the physiological responses to the stresses of warming and variations in N availability. We observed the same growth patterns at all temperatures, with the highest cell abundance in N+ and the lowest in N– conditions (Fig. 1). The cell abundances were significantly different in respect to varying N and temperature treatments ($P<0.05$, Tukey post-hoc test; Supplementary Table S1).

The highest abundance was recorded for cultures grown at 15 °C in N+ medium, 8.58 ± 0.11 × 10^7 cells l^{-1} (Fig. 1A; Supplementary Table S2). N+ medium yielded the highest cell abundances at all examined temperatures, while cells were least abundant in N– conditions ($P<0.05$, Tukey post-hoc test; Supplementary Table S1A). However, the highest maximum specific growth rates were observed at 25 °C (Table 1), while the lowest were observed at 15 °C for all conditions ($P<0.05$, Tukey post-hoc test; Supplementary Table S1B).

We observed elongation of the setae in cultures grown in N– medium relative to N± and N+ cultures ($P<0.05$, Tukey post-hoc test; Supplementary Table S1D; Fig. 2; Supplementary Table S3). At 15 °C, the setae in the N– culture were on average 3.1 µm and 3.6 µm longer than those of the N± and N+ cultures, respectively. At 25 °C, the mean differences were 7.3 µm and 7.2 µm, respectively. Setae lengths did not differ significantly between N± and N+ media (Fig. 2D). Data obtained for cultivation at 30 °C were insufficient for analysis due to the low abundance and even absence of setae (Fig. 2C).

Effect of warming and N availability on C. pseudocurvisetus *metabolism*

Chl a biosynthesis

Chl *a* concentration, expressed per cell (pg $cell^{-1}$), increased the most with temperature increase ($P<0.05$, Tukey post-hoc test, Supplementary Table S1E; Fig. 3A; Supplementary Table S4). As shown in Fig. 3B, there was a statistically significant decrease in the cell C:Chl *a* with a temperature increase from 15 °C to 25 °C for all cultures ($P<0.05$, Tukey post-hoc test; Supplementary Table S1F; Supplementary Table S4). The difference in cell C:Chl *a* between N+, N±, and N– cultures was greatest at 15 °C and cell C:Chl *a* decreased with increasing temperature, finally converging to ~54 at 30 °C. This trend was caused by both the increase of Chl *a* and the decrease in cellular C content with increasing temperature ($P<0.05$, Tukey post-hoc test, Supplementary Table S1C).

Nutrient uptake

Chaetoceros pseudocurvisetus assimilated varying amounts of DIN and PO_4^{3-} depending on the growth conditions. The general

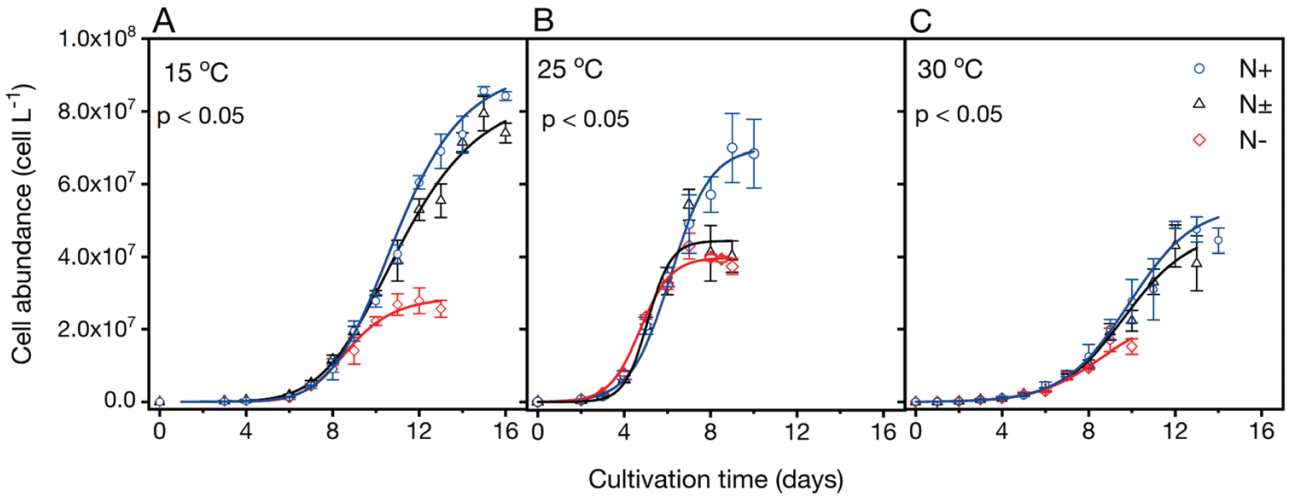

Fig. 1. Growth curves of *C. pseudocurvisetus* at (A) 15 °C, (B) 25 °C, and (C) 30 °C in N-excess (N+), optimal (N±), and N-limiting (N–) medium. Growth curves were obtained by fitting a sigmoidal curve based on plotted mean cell counts of triplicates; error bars represent the SD. *P*-values refer to two-way ANOVA results for the interaction of temperature and N availability influences on cell abundance. *P*-values for all temperature and N availability (N+, N±, and N–) combinations relating differences in cell abundances (Tukey post-hoc test) are given in Supplementary Table S1A.

Table 1. Physiological characteristics of the early stationary growth phase of *Chaetoceros pseudocurvisetus*: maximum specific growth rate (MSGR), cell volume, and cellular C content for growth in N-excess (N+), optimal (N±), and N-limiting (N–) media at 15, 25, and 30 °C

Medium	Temperature °C	MSGR (d^{-1})	Cell volume (μm^3)	Cell C content (pg C $cell^{-1}$)
N+	15	0.63 ± 0.01	2867 ± 546	183.0 ± 28.6
	25	1.02 ± 0.02	1550 ± 346	111.1 ± 20.0
	30	0.66 ± 0.02	1306 ± 143	96.9 ± 8.6
N±	15	0.62 ± 0.00	3522 ± 381	216.6 ± 19.1
	25	1.02 ± 0.00	1150 ± 22	87.4 ± 1.3
	30	0.65 ± 0.01	1613 ± 180	115.0 ± 10.4
N–	15	0.59 ± 0.03	2285 ± 239	152.5 ± 13.0
	25	1.03 ± 0.03	1364 ± 385	100.0 ± 22.7
	30	0.62 ± 0.03	1209 ± 352	90.6 ± 21.6

trend was that a greater proportion of the total amount of DIN was taken up by cells exposed to a higher initial concentration of DIN (Table 2; Supplementary Table S5). An effect of temperature on the amount of DIN taken up was observed for N+ and N± cultures, for which the decrease in N uptake paralleled the increase in temperature ($P<0.05$, Tukey post-hoc test, Supplementary Table S1G). The rate of DIN uptake was highest at 25 °C for N+ and N± cultures, and at 30 °C for N– cultures. A nearly constant PO_4^{3-} uptake rate of 0.01–0.02 pmol $cell^{-1}$ d^{-1} was observed for all cultivation treatments (Table 2).

The percentage of DIN and PO_4^{3-} taken up by *C. pseudocurvisetus* also depended on the growth temperature (Fig. 4A, B). With increasing temperature there was a statistically significant decrease in DIN uptake from 76.2 ± 10.6% to 27.1 ± 9.3% in N+ cultures and from 99.2 ± 0.2% to 56.8 ± 4.8% in N± cultures ($P<0.05$, Tukey post-hoc test, Supplementary Table S1G). The cells from the N+ medium were unable to utilize very high DIN concentrations. Because of the very low initial concentrations of DIN in N– cultures, the cells consumed almost all of the DIN, even at 30 °C. Cells grown in N+ medium utilized the most PO_4^{3-}, but showed a decreasing trend with increasing temperature, from 85.8 ± 3.4% at 15 °C to 43.4 ± 3.0 % at 30 °C ($P<0.05$, Tukey post-hoc test, Supplementary Table S1H; Fig. 4B). There was a decrease in PO_4^{3-} uptake with increasing temperature also for the N+ and N± cultures. The least PO_4^{3-} was taken up by cells in N– medium: 17.9 ± 7.5%, 15.0 ± 2.5%, and 7.0 ± 3.5% at 15, 25, and 30 °C, respectively.

The DIN:PO_4^{3-} uptake ratio varied greatly depending on the culture medium (Fig. 4C; Supplementary Table S5). In N± cultures it was almost equal for all cultivation temperatures, and varied around 20.7, slightly higher than the Redfield ratio

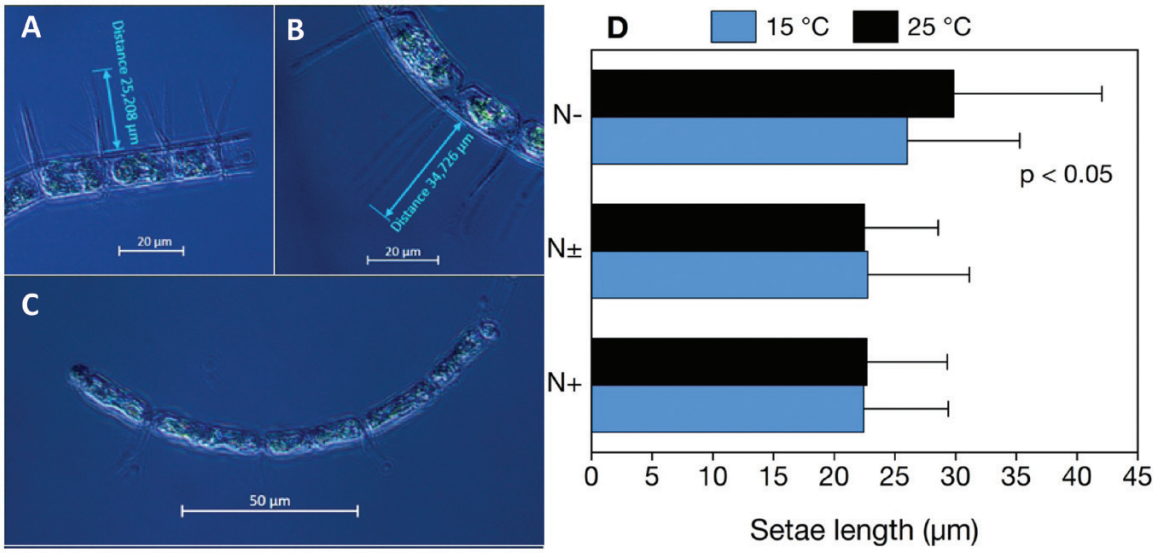

Fig. 2. Dependence of *C. pseudocurvisetus* setae length (µm) on growth conditions. (A–C) Photomicrographs of cells and their setae grown in optimal (A) and N-limiting (B) conditions at 25 °C, and cells lacking setae grown at 30 °C (C). (D) Measured setae length on cells grown under different N availability at 15 °C and 25 °C. Values presented are means of triplicates; error bars represent the SD. *P*-values refer to two-way ANOVA results for the interaction of temperature and N availability influences on cell setae length. *P*-values for the effects of all temperature and N availability (N+, N±, and N–) combinations on setae length (Tukey post-hoc test) are given in Supplementary Table S1D.

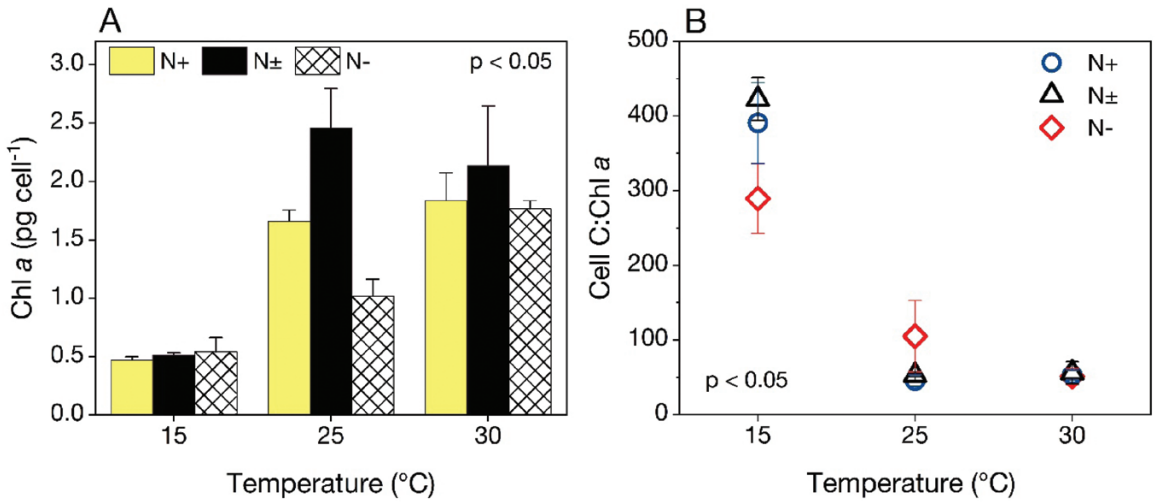

Fig. 3. Changes in the cellular Chl *a* concentration of *C. pseudocurvisetus*. Cellular concentrations of Chl *a* (pg cell^{-1}) (A) and cell C:Chl *a* (B) for N-excess (N+), optimal (N±), and N-limiting (N–) cultures of *C. pseudocurvisetus* cultures at 15, 25, and 30 °C. Values presented are means of triplicates; error bars represent the SD. *P*-values refer to two-way ANOVA results for the interaction of temperature and N availability influences on the cell content of Chl *a* and cell C:Chl *a*. *P*-values for the effects of all temperature and N availability (N+, N±, and N–) combinations on differences in the cell content of Chl *a* and cell C:Chl *a* (Tukey post-hoc test) are given in Supplementary Table S1E, F.

(16:1). Cells grown in N+ medium at 15 °C had the highest DIN:PO_4^{3-} uptake ratio (44.3 ± 6.0) (P<0.05, Tukey post-hoc test, Supplementary Table S1I). The DIN:PO_4^{3-} uptake ratio for N+ the condition decreased to 25.2 ± 1.4 at 30 °C. As expected, the lowest DIN:PO_4^{3-} uptake ratios were observed for cells grown under N– conditions at 15 °C and 25 °C, while the ratio increased to 24.7 at 30 °C. It appears that at 30 °C the DIN:PO_4^{3-} uptake ratio converges to the same value (~25) for all three N conditions.

Total organic carbon production

Total organic C produced by *C. pseudocurvisetus* cultures consists of particulate and dissolved fractions. The fact that the production of both particulate and dissolved C in N+ and N± cultures was very similar at 15 °C and 30 °C, but differed greatly at 25 °C, suggests that the growth of N± culture was terminated too early (Fig. 1B). The bulk POC concentration generally decreased with increasing temperature (P<0.05, Tukey post-hoc test, Supplementary Table S1N), whereas

Table 2. Total DIN and PO_4^{3-} taken up and their uptake rates in the early stationary growth phase of *C. pseudocurvisetus* grown in N-excess (N+), optimal (N±), and N-limiting (N–) conditions and at 15, 25, and 30 °C

Condition	T (°C)	Uptake					Uptake rate	
		DIN (pmol cell^{-1})	SD	PO_4^{3-}	SD	Culture age (d)	DIN (pmol cell^{-1} d^{-1})	PO_4^{3-}
N+	15	6.79	±0.99	0.15	±0.00	16	0.42	0.01
	25	5.87	±1.28	0.18	±0.01	10	0.59	0.02
	30	3.46	±1.52	0.14	±0.01	13	0.27	0.01
N±	15	3.23	±0.12	0.17	±0.01	16	0.20	0.01
	25	3.87	±0.99	0.18	±0.05	8	0.48	0.02
	30	3.70	±0.47	0.18	±0.03	13	0.28	0.01
N–	15	1.32	±0.38	0.12	±0.06	14	0.09	0.01
	25	0.81	±0.05	0.06	±0.01	9	0.09	0.01
	30	2.24	±0.34	0.07	±0.03	10	0.22	0.01

Results on two-way ANOVA tests are given in Supplementary Tables S1J, K, L, M.

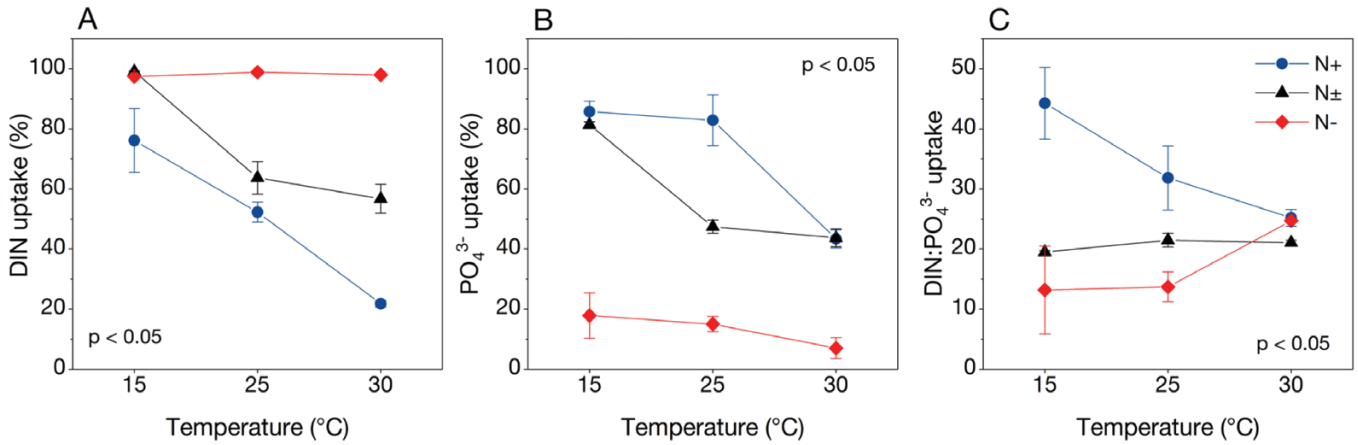

Fig. 4. *Chaetoceros pseudocurvisetus* nutrient uptake. Percentage of DIN (A) and PO_4^{3-} (B) uptake based on the amount of nutrients depleted from the media from the beginning until the early stationary growth phase in each experimental batch, and DIN:PO_4^{3-} uptake ratio per cell (C) for growth at 15, 25, and 30 °C in N-excess (N+), optimal (N±), and N-limiting (N–) conditions. Values presented are means of triplicates; error bars represent the SD. *P*-values refer to two-way ANOVA results for the interaction of temperature and N availability influences on DIN, PO_4^{3-}, and DIN: PO_4^{3-} uptake. *P*-values for the effects of all temperature and N availability (N+, N±, and N–) combinations on differences in nutrient uptake data (Tukey post-hoc test) are given in Supplementary Table S1G–I.

opposite trends were observed for DOC production but were not statistically significant (Tukey post-hoc test, Supplementary Table S1O; Figs. 5A, B; Supplementary Table S6).

POC normalized to cell concentration ranged from 205.9 ± 9.4 pg C cell^{-1} to 211.4 ± 23.1 pg C cell^{-1} for the N+ culture, 213.7 ± 27.3 pg C cell^{-1} to 252.0 ± 36.9 pg C cell^{-1} for the N± culture, and 223.7 ± 7.4 pg C cell^{-1} to 271 ± 46.5 pg C cell^{-1} for the N– culture (Fig. 5C; Supplementary Table S6). The share of cellular C (Table 1) in POC (%) was calculated to determine the proportion of C in the particulate fraction that belongs to the active biomass, since a certain amount of POC content corresponds to dead cells (non-living POC) and particular organic matter that leaked out of the dead cells. Cellular C in POC (%) (Fig. 5D; Supplementary Table S6) decreased with increasing temperature ($P<0.05$, Tukey post-hoc test, Supplementary Table S1R) and was lowest for the N– cultures. Of the two stressors, the increase in temperature had the greater effect on the increase in the percentage of non-living POC, indicating high cell mortality. Cellular C in POC (%) decreased from 88.7 ± 12.1, 97.0 ± 10.4, and 72.8 ± 14.1 at 15 °C to 46.0 ± 3.7, 37.5 ± 9.2, and 35.7 ± 4.4 at 30 °C for the N+, N±, and N– cultures, respectively.

Because of the much higher microbial degradation rates of POC compared with DOC degradation (Attermeyer *et al.*, 2018), the DOC content per cell increased in parallel with the increased content of non-living POC ($P<0.05$ for N+ and N±, ANOVA; for N– there was a positive but non-significant trend) (Fig. 5E; Supplementary Table S6). The highest value of DOC, 97.5 ± 26.1 pg C cell^{-1}, was observed for the N– condition at 30 °C ($P<0.05$, Tukey post-hoc test; Supplementary Table S1S).

Lipid production

We processed data for cellular lipids (CL) produced by the *C. pseudocurvisetus* cultures, including membrane (PL, GL, and ST) and storage (TG and SE) lipids (Figs. 6). Bulk concentra-

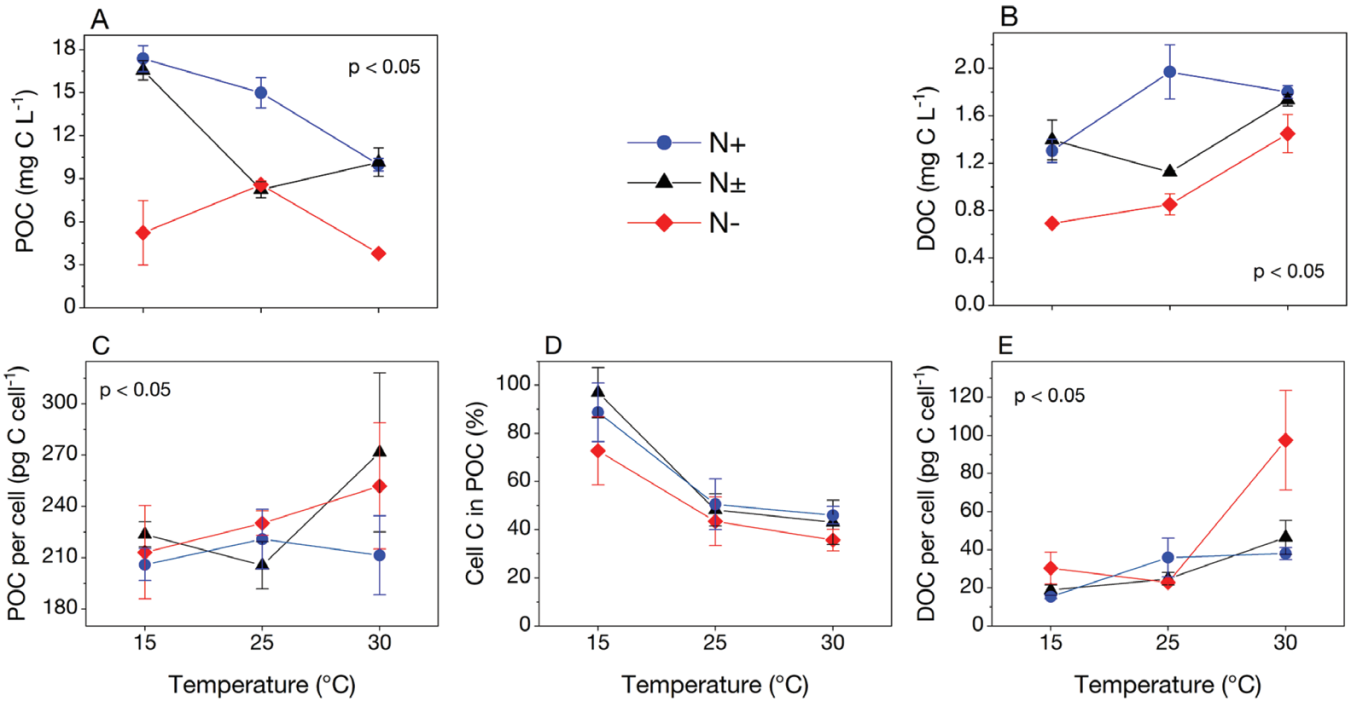

Fig. 5. Organic carbon production as a function of N availability and temperature. Particulate organic carbon (POC) (mg C l^{-1}) (A), dissolved organic carbon (DOC) (mg C l^{-1}) (B), POC normalized to cell (pg C $cell^{-1}$) (C), cellular carbon in POC (%) (D), and DOC normalized to cell (pg C $cell^{-1}$) (E). Values presented are means of triplicates; error bars represent the SD. *P*-values refer to two-way ANOVA results for the interaction of temperature and N availability influences on organic carbon data. *P*-values for the effects of all temperature and N availability (N+, N±, and N–) combinations on differences in organic carbon data (Tukey post-hoc test) are given in Supplementary Table S1N–P, R.

tions of CL decreased with increasing temperature and with decreasing N availability in the culture medium ($P<0.05$, two-way ANOVA, Supplementary Table S1T; Fig. 6A). The highest CL concentration was detected at 15 °C for N+ cultures (1.33 ± 1.5 mg l^{-1}) and the lowest for N–cultures at 30 °C (0.44 ± 0.05 mg l^{-1}) (Supplementary Table S7). The CL content per cell (pg $cell^{-1}$) increased with temperature ($P<0.05$, two-way ANOVA, Supplementary Table S1T), and was highest for N– cultures at all three temperatures (ranging from 22.6 ± 2.4 to 29.2 ± 1.5 pg $cell^{-1}$). Depite the observed trend, it was not statistically significant (Tukey post-hoc test, Supplementary Table S1U; Fig. 6B).

The relative quantities of CL classes changed as a function of increasing temperature and N availability in the medium (Fig. 6C–E; Supplementary Table S8). The most abundant were GL (MGDG+DGDG+SQDG), which accounted for 34–52% of CL. The relative proportions of lipid classes (%) of *C. pseudocurvisetus* grown at 15 °C were not significantly different between the N+, N±, and N–cultures. PC and TG differed significantly in respect to N availability at 25 °C, while MGDG, DGDG, SQDG, PE, and TG differed significantly at 30 °C. The proportion of MGDG and DGDG in CL decreased from N+ to N– media at 30 °C, while the opposite trend was observed for SQDG and TG. The contribution of MGDG to CL decreased almost 2-fold from 26.07 ± 6.26% at 15 °C to 14.11 ± 2.45% at 30 °C in N– medium.

The quantities of the thylakoid lipids SQDG and DGDG were positively correlated with temperature, whereas the storage lipids TG and SE exhibited a negative correlation with the initial DIN concentration in the medium. Thus, the percentage of TG in CL was highest in N–, amounting to 10.17 ± 0.69% irrespective of growth temperature. The contribution of SE to CL was mainly less than 1%, except in the N– cultures at 30 °C (1.1 ± 0.6%). Relevant statistical results are presented in Supplementary Tables S9, S10.

Total protein production

The effects of warming and N stresses on *C. pseudocurvisetus* growth were reflected in the observed decrease in bulk protein concentration (Fig. 7A; Supplementary Tables S11, S12); this decrease was statistically significant for the N+ and N± cultures ($P<0.05$, Tukey post-hoc test, Supplementary Table S1V). The highest bulk protein concentrations were found for the N+ cultures, 9.84 ± 0.91 mg l^{-1}, 8.27 ± 0.07 mg l^{-1}, and 5.90 ± 0.59 mg l^{-1} at 15, 25, and 30 °C, respectively. Bulk protein concentrations were lowest for the N– cultures, and these did not differ significantly among the three temperature cultivations, ~2.10 mg l^{-1}. Data on the cellular protein content of *C. pseudocurvisetus* are shown in Fig. 7B and Supplementary Table S11. The highest content, observed at 30 °C, should be taken with caution, since undecomposed particulate proteins of dead cells probably contributed to the total proteins.

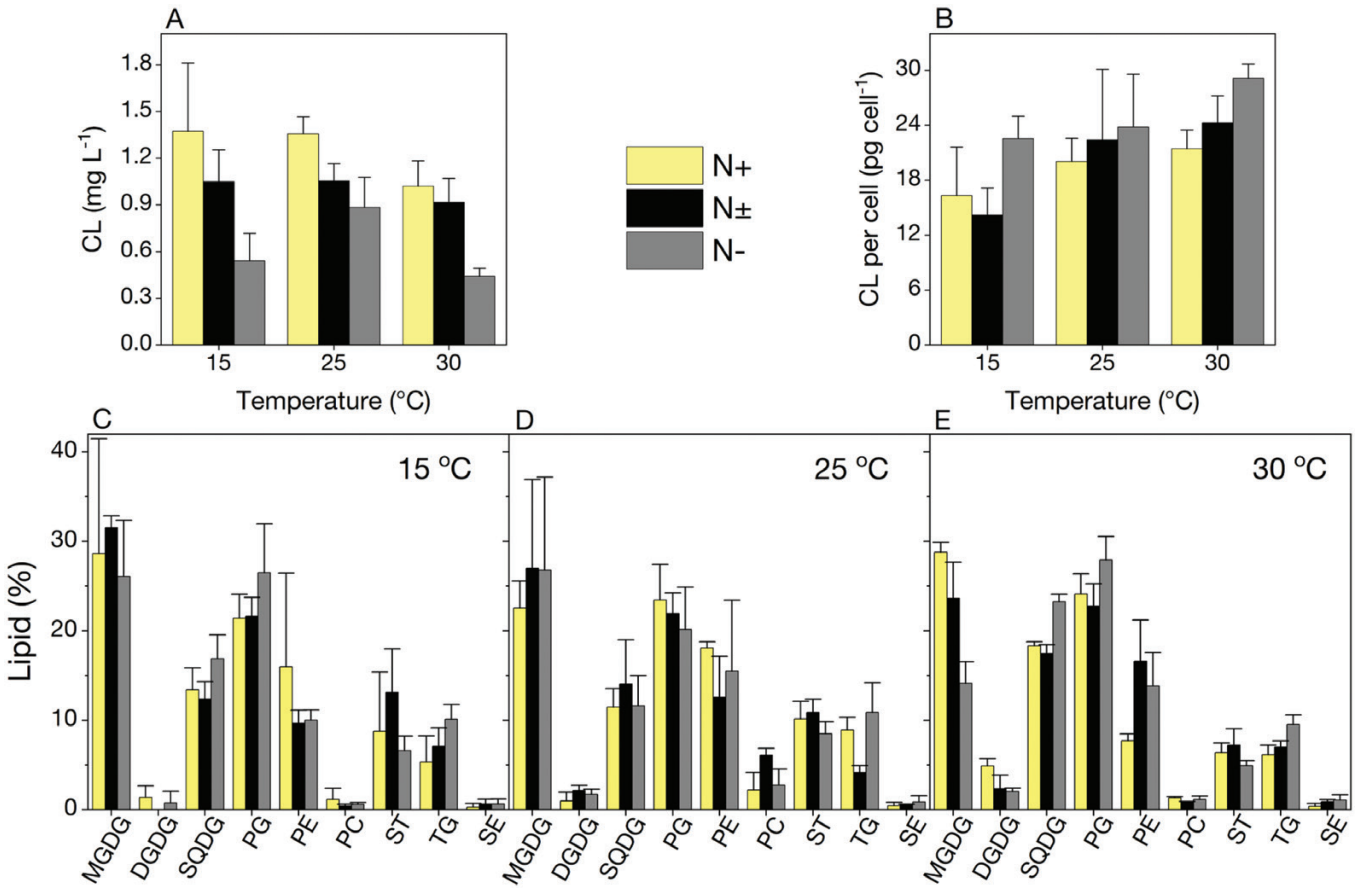

Fig. 6. *Chaetoceros pseudocurvisetus* lipid production. Bulk cellular lipids (CL) (mg l^{-1}) (A), CL normalized to cell (pg $cell^{-1}$) (B), and proportions of lipid classes to cell lipids (%) for the N-excess (N+), optimal (N±), and N-limiting (N–) cultures at 15 °C (C), 25 °C (D), and 30 °C (E). Lipid classes: monogalactosyldiacylglycerols (MGDG), digalactosyldiacylglycerols (DGDG), sulfoquinovosyldiacylglycerols (SQDG), phosphatidylglycerols (PG), phosphatidylethanolamines (PE), phosphatidylcholines (PC), sterols (ST), triacylglycerols (TG). and steryl esters (SE). Values presented are means of triplicates; error bars represent the SD.

One should also consider that the cells were dividing less frequently at 30 °C and that they retained their cellular protein content. Statistically significant differences in cellular content of proteins were detected for the N– condition ($P<0.05$, Tukey post-hoc test, Supplementary Table S1W). The highest protein:CL ratio was detected for *C. pseudocurvisetus* growing in N± medium at 15 °C (9.49 ± 1.48), and this value was significantly higher than that at 25 °C ($P<0.05$, Tukey post-hoc test, Supplementary Table S1X; Fig. 7C). We observed no significant differences in the protein:CL ratio of the cultures at 30 °C and for the three different N treatments at this temperature (Supplementary Table S1X; Supplementary Table S12). The ratios were 5.49 ± 1.64, 5.94 ± 0.90, and 4.55 ± 0.48 for the N+, N±, and N– cultivations, respectively. An interesting observation is that for the N– cultures, on average the highest protein:CL ratio was observed for the culture at 30 °C. It seems that protein:CL ratios at 30 °C converge to the same value of ~5.3.

Discussion

Physical and chemical conditions in the marine environment have a major influence on the physiology of phytoplankton and the distribution of cellular resources. Physiological and biochemical changes in phytoplankton can lead to shifts in community structure and trophic interactions that affect entire marine ecosystems. The Anthropocene era has already profoundly altered the global ocean. There is indisputable evidence of a variety of changes in the marine ecosystem due to global changes such as warming and oligo- and eutrophication. Temperatures in the Mediterranean Sea are continuously rising (Lejeusne *et al.*, 2010). Summer temperatures in the surface waters of the Adriatic Sea, for example, frequently approach and even exceed 30 °C (Gašparović, 2012). The Mediterranean Basin is experiencing more frequent heat waves of increasing duration (Cramer *et al.*, 2018). The nutrient budget of the Mediterranean Basin is expected to decrease in the

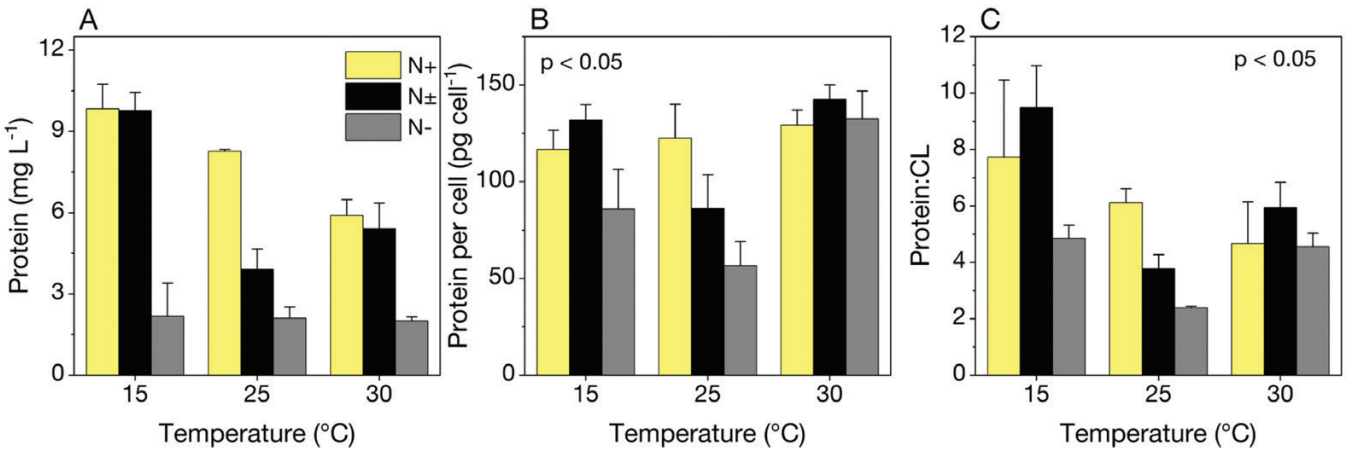

Fig. 7. *Chaetoceros pseudocurvisetus* protein production. Bulk protein (A) and protein concentrations normalized to cell (B), and protein:cellular lipid (CL) ratio (C). Data are presented for the cultures grown at 15, 25, and 30 °C and in N-excess (N+), optimal (N±), and N-limiting (N–) conditions. Values presented are means of triplicates; error bars represent the SD. *P*-values refer to two-way ANOVA results for the interaction of temperature and N availability influences on cellular protein content and protein:CL ratio. *P*-values for the effects of all temperature and N availability (N+, N±, and N–) combinations on differences in cellular protein content and protein:CL ratio (Tukey post-hoc test) are given in Supplementary Table S1W, X.

northwestern basin and the Adriatic Sea, while it could increase sharply in the basins of the southern and northern Levantine Seas (Ludwig *et al.*, 2010). Recently, N limitation has been observed more frequently in the northern Adriatic Sea (Penezić *et al.*, 2022). Against this background, in the present study, we investigated the whole-cell response of the diatom *C. pseudocurvisetus* to warming and variable N supply. A summary of the main observed morphological, physiological, and biochemical responses of *C. pseudocurvisetus* to high temperature and availability of inorganic N is shown in Fig. 8.

C. pseudocurvisetus *physiological and morphological acclimation*

The abundance and growth dynamics of *C. pseudocurvisetus* were influenced by both warming and N availability. However, N depletion has a stronger negative effect on total abundance than warming (Fig. 1; Supplementary Table S1A; Supplementary Table S2). Aranguren-Gassis *et al.* (2019) found that the marine diatom *Chaetoceros simplex* survives high temperatures in N abundance, whereas N limitation inhibits its adaptation to high temperatures. Optimal growth temperature allows cells to undergo photosynthesis without modifying inherent biochemical or physiological properties (Ras *et al.*, 2013) and thereby produce a large amount of biomass (Sharma *et al.*, 2012). Cultures of *C. pseudocurvisetus* growing at sufficient DIN concentrations (N+ and N±) and at 15 °C, which is considered to be the optimal temperature for this species (Novak *et al.*, 2018), reached their maximum abundance. An increase in temperature (below the sustainable maximum growth temperature) has a positive effect on photosynthesis and growth rates, mainly through increased enzymatic activities (Falkowski, 1980). Excessive temperature (30 °C) leads to high cell mortality (Fig. 5D). Here, the specific growth rate increased until 25 °C and decreased at 30 °C, suggesting that the upper thermal limit for this species is between 25 °C and 30 °C (Fig. 1; Supplementary Table S1). This finding suggests that *C. pseudocurvisetus* would adapt well to the increasingly warm conditions of the Mediterranean Sea until the upper thermal limit is reached. When the temperature threshold is exceeded, the growth rate of microalgae decreases due to heat stress, which likely triggers the denaturation of enzymes and proteins involved in important metabolic processes (Chen, 2015). *Chaetoceros pseudocurvisetus* isolated from the Sagami Bay (*in situ* temperature 25 °C) survives in a narrow temperature range (20–30 °C) (Suzuki and Takahashi, 1995). In contrast, *C. pseudocurvisetus* isolated from the Adriatic Sea appears to survive in a wider temperature range, as it survives and reproduces from at least 10 °C to 30 °C. These varying findings suggest a high evolutionary potential of this species, reflected in strong local adaptations.

The observed elongation of *C. pseudocurvisetus* setae (Fig. 2D; Supplementary Table S1D; Supplementary Table S3) suggests a previously unobserved morphological plasticity in response to N limitation. Smodlaka Tanković *et al.* (2018) reported a remarkable morphological strategy in response to nutrient limitation in *Chaetoceros peruvianus*, namely the thickening and elongation of setae of cells grown in a P-limited environment. They showed increased extracellular alkaline phosphatase activity upon P limitation and, interestingly, alkaline phosphatase was exclusively localized in the setae. This morphological change increased the surface area for alkaline phosphatase activity and enhanced the ability of the species to utilize dissolved organic P when environmental PO_4^{3-} concentrations are low. In contrast to the thick setae of *C. peruvianus*, the weakly silicified setae of *C. pseudocurvisetus* are thin (diameter 0.7–1.4 μm; Lee *et al.*, 2014). The presence of extracellular enzymes on the

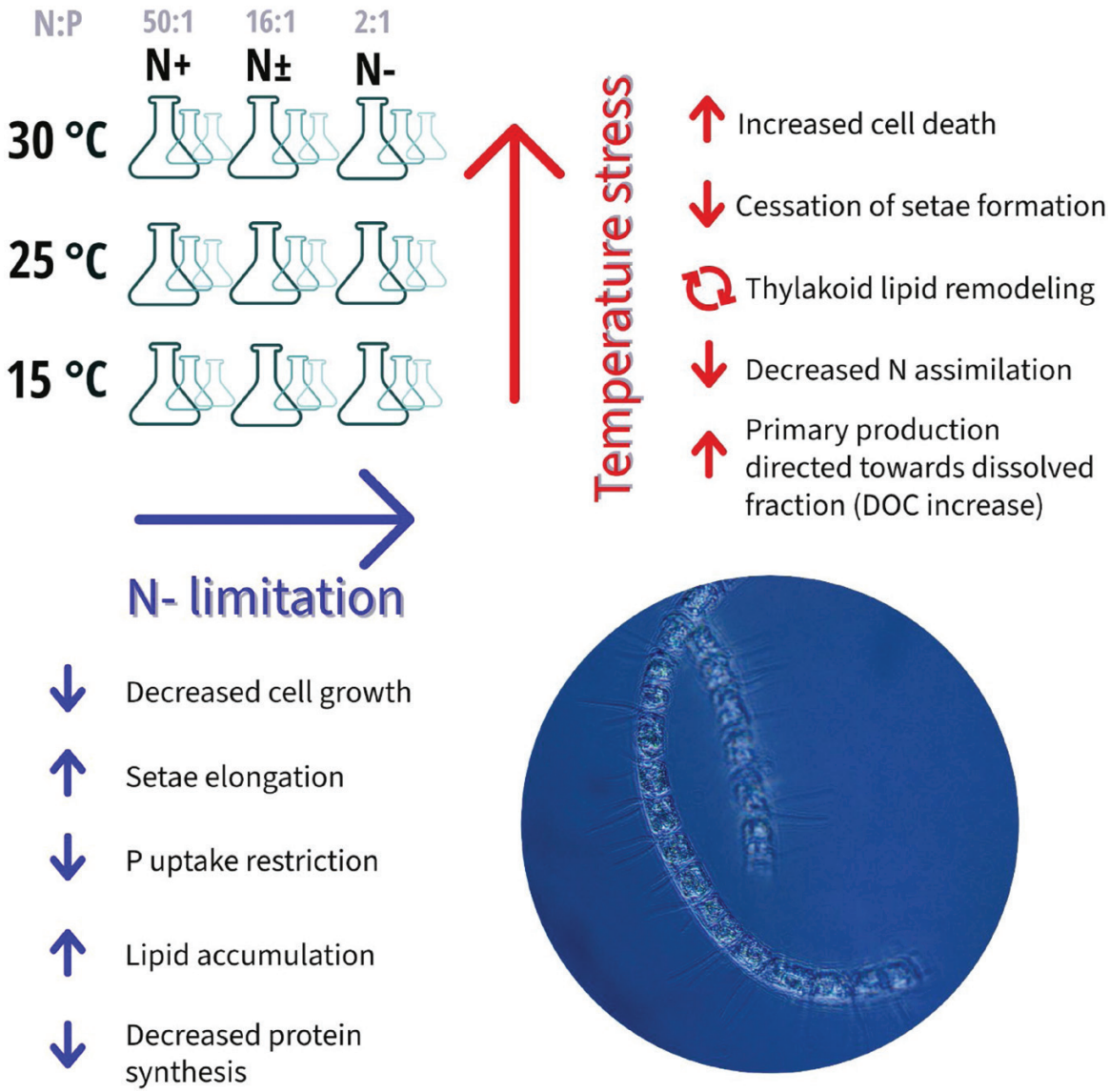

Fig. 8. Diagram highlighting the most important findings of the study.

setae as a mechanism to enhance N uptake could explain the elongation of the setae. Phytoplankton can produce cell-surface-attached amino acid oxidase and amine oxidase to use different forms of organic N (Palenik *et al.*, 1989). Setae are assumed to increase the absorptive surface of the cell (Margalef, 1978). Thus, the elongation of setae of smaller cells growing under N– conditions could represent a strategy to increase the surface area for inorganic N uptake, as an energy cost alternative to cell growth and reproduction. The growth and elongation of the setae was massively reduced at 30 °C (Fig. 2C). We assume that setae growth is suppressed at this temperature as resources are redirected to support essential metabolic processes and extend survival. This phenomenon is likely to have consequences for the diatom in a real ecosystem. Setae provide buoyancy and positioning of the diatoms in the water column (Gómez, 2020) and mechanical protection from grazers (Hamm *et al.*, 2003). Thus, the 'setaeless' condition in warm waters leads to greater ecological vulnerability of diatoms, as they are at greater risk from sinking and grazing. The former could facilitate downward export of organic matter, while the latter, in contrast, may enhance remineralization in the upper mixed layer of the water. However, both factors may lead to a decline in the abundance of *C. pseudocurvisetus* and analogous species at high sea-surface temperatures such as 30 °C.

C. pseudocurvisetus *biochemical acclimation*

The observed increase in Chl *a* content and decrease in cell C:Chl *a* that follow the increase in temperature (Fig. 3; Supplementary Table S1E, F; Supplementary Table S4) could be

explained by the fact that cells respond to a temperature increase by investing in Chl *a* synthesis to obtain energy for the physiological processes necessary for survival. Since photosynthesis produces carbohydrates that have obviously not been used to increase the C content of the cell (low cell C:Chl *a*), they are probably excreted to the dissolved fraction of primary production. Indeed, we observed a sharp increase in DOC with increasing temperature (Figs. 5B, E; Supplementary Table S1O; Supplementary Table S6). Nutrient availability appeared to be less influential on cellular C and Chl *a* content than high temperature (Supplementary Table S1C, E). N limitation is reported to elevate phytoplankton cell C:Chl *a* (Geider, 1987). In contrast, we found an inconsistent effect of N deficiency on cell C:Chl *a* (Fig. 3B; Supplementary Table S4). Growth conditions largely reflect on internal biochemistry. Temperature has a major influence on the rate of photosynthesis (Davidson, 1991) and thus it is an important driver of the production and transformation of key macromolecules in phytoplankton (Lee *et al.*, 2017) However, Chl *a* and primary production are either limited or stimulated in the optimal temperature range by nutrient availability in the environment (Davey *et al.*, 2008).

Nutrient (DIN and PO_4^{3-})uptake by cells depends greatly on the DIN concentration in the medium and increases with the increasing initial N concentration (N+>N±>N–) (Table 2). This is consistent with the results from a study by Lomas and Gilbert (2000) in which all diatom species studied had the capability to continue taking up NO_3^- at increasing rates with increased NO_3^- concentration. While total acquired N relative to the initial concentration decreased with increasing temperature, as the main negative influential factor (Fig. 4A, B), the response of the DIN uptake rate to increasing temperature in N+ and N± cultures showed a pattern similar to that of the growth rate, that is, the uptake rate was highest at 25 °C (Table 2). The highest DIN uptake rates at 30 °C of the N– cultures is likely due to the energy savings of less important cellular processes, such as the observed cessation of setae formation (Fig. 2C). There is an apparent discrepancy between the results indicating (i) increased cellular uptake rates and (ii) a decreased amount of DIN taken up from the medium with increasing temperature. It appears that even as the uptake rate of DIN increases with increasing temperature, the maximum cell density decreases, resulting in an overall decrease in the consumption of DIN relative to its initial concentration in the medium.

N deficiency limits P acquisition, which is why less than 20% of P is taken up by N– cultures (Fig. 4B; Supplementary Table S5). The observed ratio of assimilated N:P differs from the Redfield ratio of 16:1. Our data suggest that a ratio of ~20:1 is the optimal N:P ratio for *C. pseudocurvisetus*, as determined for the optimal culture (N±) at all temperatures (Fig. 4C; Supplementary Table S5). Interestingly, when temperature was optimal and N was abundant (N+ cultures, 15 °C), the incorporated ratio was on average 44.3. This indicates the formation of N reserves in the cell. In conditions of N surplus, diatoms store N in the form of proteins, amino acids, and nitrate (Dortch, 1982). Our data on protein:CL ratio (Fig. 7C; Supplementary Table S11) suggest that *C. pseudocurvisetus* stores excessively assimilated N in the form of proteins. The uptake of PO_4^{3-} is also inhibited with increasing temperature (Fig. 4B; Supplementary Table S1H; Supplementary Table S5) and seems to be even more suppressed compared with N uptake under N– conditions, which we inferred from the increase in the N:P ratio at 30 °C compared with 15 °C and 25 °C, from on average 13.4, as observed at 15 °C and 25 °C, to 24.7 at 30 °C.

Increasing stress (warming and N limitation) is reflected in the lower POC concentration in the medium, which is accompanied by the reduced number of cells (Fig. 1; Fig. 5A, C; Supplementary Table S6). At the same time, increasing stress is accompanied by an increase in DOC concentration (Fig. 5B, E). The decreased contribution of cellular C to POC at high temperature and in N– cultures (Fig. 5D; Supplementary Table S6), coupled with reduced cell abundance, suggests substantial cell die-off under stressful conditions, with high primary production directed toward the dissolved fraction. Our data suggest that unfavourable temperature has a stronger effect on *C. pseudocurvisetus* cell death than lack of N.

Higher bulk lipid concentrations can be expected in cultures with higher cell abundance. While the bulk lipid concentration is lowest, the accumulation of lipids per cell is the greatest in cultures grown at 30 °C, especially in N– cultures (Fig. 6A; Supplementary Table S1U; Supplementary Table S7). The individual effects of temperature increase and particularly N limitation cause a significant accumulation of cell lipids, while the combination of the two stressors results in the highest CL content.

Lipid composition varies depending on environmental conditions and represents mechanisms of acclimation and adaptation. The marine diatom *Thalassiosira pseudonana* replaces PC with betaine lipids and PG with SQDG depending on P availability (Martin *et al.*, 2011). The composition of PL fatty acids changes depending on estuarine conditions (Vrana Špoljarić *et al.*, 2021). Here, the observed statistically significant increase in the proportion of DGDG and SQDG in the cells with increasing temperature (Supplementary Table S9) can be explained by their role in thylakoid membranes and in achieving thermotolerance (Sato *et al.*, 2003; Chen *et al.*, 2006; Mizusawa *et al.*, 2009). Lipids of thylakoid membranes, where the early processes of photosynthesis occur (Murata and Siegenthaler, 1998), play important roles in the folding and assembly of protein subunits in photosynthetic complexes (Kobayashi *et al.*, 2016). Photosynthesis is very sensitive to high-temperature stress. The primary sites of targets of high-temperature stress are Photosystem II (PSII) and Rubisco (Mathur *et al.*, 2014). Bilayer-forming DGDG lipids are particularly present in the PSII complex (Mizusawa *et al.*, 2013), shaping the final structure of PSII (Boudière *et al.*, 2014). SQDGs are dominantly localized in the PSII core complex and PSII light-harvesting complex (Sato *et al.*, 1995). The observed increase in both DGDG and SQDG at 30 °C (Fig. 6E) could be explained by

the role of DGDG in balancing the electrostatic repulsion between negatively charged SQDG, as observed by Demé *et al.* (2014), who performed *in vitro* experiments on reconstituted thylakoid lipid extracts. This should serve to achieve thermotolerance. The observed reduction of non-bilayer-forming MGDGs at high temperature and in N-deficient conditions (Fig. 6E) may be explained by the role of the DGDG:MGDG ratio in stabilizing the newly adjusted thylakoid membrane, as observed for Arabidopsis (Gaude *et al.*, 2007) and the thermotolerant reef coral symbiont dinoflagellate *Durusdinium trenchii* (Rosset *et al.*, 2019). Finally, these results clearly suggest reorganization of the photosynthetic apparatus under the influence of stressors. In particular, high temperature significantly affects lipid remodelling.

Intracellular N is distributed among proteins and amino acids, chlorophylls, RNA, DNA, and inorganic N. The distribution is strongly influenced by growth conditions. Proteins are the most important N-containing substances [59.3–96.8% of total cellular N (TN)], followed by inorganic N (0.4–30.4% of TN), nucleic acids (0.3–12.2% of TN), and chlorophylls (0.1–1.8% of TN) (Lourenço *et al.*, 2004). Considering that proteins are particularly sensitive to temperature stress, the observed increase of cellular protein content in the N+ and N– cultures at 30 °C is unexpected. However, under warmer temperatures, *Chaetoceros* sp. invest in chaperones and folding catalysts that help to reduce endoplasmic reticulum stress, and the investment of peptidases and proteasomes can promote the removal of misfolded proteins in the endoplasmic reticulum and support faster protein turnover (Liang *et al.*, 2019). Furthermore, Sheehan *et al.* (2020) found that the diatom *T. pseudonana* exhibits increased protein content over the temperature range of 14–28 °C. Temperature adaptation is based on changes in the expression of targeted genes and pathways to maintain normal cellular functions (Liang *et al.*, 2019). Photosynthetic complexes are highly dependent on the balanced cooperation of thylakoid lipids with embedded protein moieties. Sato *et al.* (2003) suggested that photosynthetic activity remains functional at high temperatures not by the stabilization of PSII activity, but rather by the reactivation of PSII after damage. Its recovery is closely related to the *de novo* synthesis of proteins encoded by the nuclear and chloroplast genomes (Sato *et al.*, 2003). We propose that at the supraoptimal temperature of 30 °C, proteins involved in the repair of heat-induced damage to PSII increase in parallel with the increase in the lipids SQDG and DGDG, which are involved in recovery.

Consideration of the protein:CL ratio gave us a good insight into cell biochemistry. Under optimal conditions in terms of the N:P ratio (16:1), cells have the highest protein:CL ratio, indicating that an optimal N:P ratio in the growth medium is important for cell health, regardless of the growth temperature. Smith *et al.* (1997) showed that lipid synthesis is favoured over protein or carbohydrate synthesis in conditions of low nutrient availability. The protein:CL ratio converged to the same value of –5.3 at 30 °C, regardless of the N availability. Since we observed the same values for all three N treatments at 30 °C for DIN:PO_4^{3-} (~25, Fig. 4C; Supplementary Table 4) and cell C:Chl *a* (~54, Fig. 3B; Supplementary Table S4), we suggest that cell biochemistry is most strongly affected by excessively high temperature.

Conclusions

Understanding phytoplankton acclimation and adaptation is critically needed for predicting future ocean/sea responses to global climate change stressors. Different phytoplankton species respond differently, among which there will be 'global winners' that will adapt to climate change. As a consequence, species-level research is of great importance.

A combination of physiological, morphological, and biochemical data gave us insight into the response of *C. pseudocurvisetus* to adverse environmental conditions, namely high temperatures as well as the excess or shortage of inorganic N. Under elevated temperatures, metabolic reactions and cell growth accelerate, until the thermal niche width of *C. pseudocurvisetus* species is exceeded (>25 °C). Key research findings include: (i) the morphological response to N limitation is setae elongation (surface area increase), which most likely increases N uptake; (ii) cessation of setae formation at 30 °C appears to be a mechanism to divert resources to support essential metabolic processes and to prolong survival; (iii) N limitation restricts P uptake; (iv) increasing temperature significantly directs the primary production to the dissolved fraction; (v) the lipids most sensitive to temperature rise are thylakoid lipids, which are significantly remodelled [altered share of DGDG and SQDG (increase) and MGDG (decrease)]; (vi) under an optimal N:P ratio (16:1) and at 15 °C, cells are the healthiest relative to N+ and N– conditions, as indicated by the highest protein:CL ratio; and (vii) even in comparison to severe N limitation, cell biochemistry is most affected by excessively high temperature.

Supplementary data

The following supplementary material is available at *JXB* online.

Table S1. Results of statistical analyses.

Table S2. Response of *C. pseudocurvisetus* growth to nitrogen availability and increasing temperature.

Table S3. Average length and abundance of measured setae.

Table S4. Changes in *C. pseudocurvisetus* cellular pigment concentration.

Table S5. *C. pseudocurvisetus* nutrient uptake.

Table S6. *C. pseudocurvisetus* total organic matter production.

Table S7. Quantitative data for cellular lipids of *C. pseudocurvisetus*.

Table S8. Quantitative data for contribution of lipid classes to cell lipids (%).

Table S9. Contribution of each lipid class to cell lipids (%) analysed for mean differences in respect to N availability at each growth temperature.

Table S10. Pearson's correlation coefficient between growth temperature, DIN concentration, and content of cellular lipid classes.

Table S11. *C. pseudocurvisetus* protein production.

Table S12. Bulk and normalized protein content and protein:cell lipid ratio analysed for significance of the mean difference between N treatments at each growth temperature.

Acknowledgements

The authors thank Dr Ana Smolko from the Laboratory for Chemical Biology, Division of Molecular Biology, Ruđer Bošković Institute, Croatia for help in protein measurement.

Author contributions

LF and BG: writing—original draft; LF: investigation, data collection, formal analysis; IV, ACK, JC, TN, and AP: investigation; BG: conceptualization, supervision, resources; all authors: writing—revision and editing. All authors read and approved the submitted version.

Conflict of interest

The authors have no conflicts of interest to declare.

Funding

This work was funded by the grants from the Croatian Science Foundation under the projects IP-2018-01-3105 and IP-11-2013-8607.

Data availability

All data supporting the findings of this study are available within the paper and within its supplementary materials published online.

References

Anning T, Harris G, Geider R. 2001. Thermal acclimation in the marine diatom *Chaetoceros calcitrans* (Bacillariophyceae). European Journal of Phycology **36**, 233–241.

Aranguren-Gassis M, Kremer CT, Klausmeier CA, Litchman E. 2019. Nitrogen limitation inhibits marine diatom adaptation to high temperatures. Ecology Letters **22**, 1860–1869.

Attermeyer K, Catalán N, Einarsdottir K, Freixa A, Groeneveld M, Hawkes JA, Jonas Bergquist J, Tranvik LJ. 2018. Organic carbon processing during transport through boreal inland waters: particles as important sites. Journal of Geophysical Research **123**, 2412–2428.

Berges JA, Charlebois DO, Mauzerall DC, Falkowski PG. 1996. Differential effects of nitrogen limitation on photosynthetic efficiency of photosystems I and II in microalgae. Plant Physiology **110**, 689–696.

Bindoff NL, Cheung WWL, Kairo JG *et al.* 2019: Changing ocean, marine ecosystems, and dependent communities. In: Pörtner H-O, Roberts DC, Masson-Delmotte V ***et al***., eds. IPCC special report on the ocean and cryosphere in a changing climate. Geneva: Intergovernmental Panel on Climate Change.

Bligh EG, Dyer WJ. 1959. A rapid method of total lipid extraction and purification. Canadian Journal of Biochemistry and Physiology **37**, 911–7.

Bopp L, Aumont O, Cadule P, Alvain S, Gehlen M. 2005. Response of diatoms distribution to global warming and potential implications: A global model study. Geophysical Research Letters **32**, n/a1–n/a.

Bosak S, Godrijan J, Šilović T. 2016. Dynamics of the marine planktonic diatom family *Chaetocerotaceae* in a Mediterranean coastal zone. Estuarine, Coastal and Shelf Science **180**, 69–81.

Boudière L, Michaud M, Petroutsos D, *et al.* 2014. Glycerolipids in photosynthesis: composition, synthesis and trafficking. Biochimica et Biophysica Acta **1837**, 470–80.

Bristow LA, Mohr W, Ahmerkamp S, Kuypers MMM. 2017. Nutrients that limit growth in the ocean. Current Biology **27**, 474–478.

Chen B. 2015. Patterns of thermal limits of phytoplankton. Journal of Plankton Research **37**, 285–292.

Chen J, Burke JJ, Xin Z, Xu C, Velten J. 2006. Characterization of the *Arabidopsis* thermosensitive mutant *atts02* reveals an important role for galactolipids in thermotolerance. Plant, Cell and Environment **29**, 1437–48.

Christie-Oleza J, Sousoni D, Lloyd M, Armengaud J, Scanlan DJ. 2017. Nutrient recycling facilitates long-term stability of marine microbial phototroph–heterotroph interactions. Nature Microbiology **2**, 17100.

Cramer W, Guiot J, Fader M, Garrabou J, Gattuso JP, *et al.* 2018. Climate change and interconnected risks to sustainable development in the Mediterranean. Nature Climate Change **8**, 972–980.

Davey M, Tarran GA, Mills MM, Ridame C, Geider RJ, La Roche J. 2008. Nutrient limitation of picophytoplankton photosynthesis and growth in the tropical North Atlantic, Limnology and Oceanography **53**, 1722–1733.

Davison IR. 1991. Environmental effects on algal photosynthesis: temperature. Journal of Phycology **27**, 2–8.

de Castro Araújo S, Garcia VMT. 2005. Growth and biochemical composition of the diatom *Chaetoceros* cf. *wighamii* brightwell under different temperature, salinity and carbon dioxide levels. I. Protein, carbohydrates and lipids. Aquaculture **246**, 405–412.

Demé B, Cataye C, Block MA, Maréchal E, Jouhet J. 2014. Contribution of galactoglycerolipids to the 3-dimensional architecture of thylakoids. FASEB Journal **28**, 3373–3383.

Dortch Q. 1982. Effect of growth conditions on accumulation of internal nitrate, ammonium, amino acids, and protein in three marine diatoms. Journal of Experimental Marine Biology and Ecology **61**, 243–264.

Falkowski PG, Woodhead AD. 1992. Primary productivity and biogeochemical cycles in the sea. Environmental Science Research, Vol. **1**. Boston: Springer.

Falkowski PG. 1980. Light-shade adaptation in marine phytoplankton. In: Falkowski PG ed. Primary productivity in the sea. Environmental Science Research, **Vol**. 19. Boston: Springer, 99–119.

Falkowski PG. 1997. Evolution of the nitrogen cycle and its influence on the biological sequestration of CO_2 in the ocean. Nature **387**, 272–275.

Gašparović B. 2012. Decreased production of surface-active organic substances as a consequence of the oligotrophication in the northern Adriatic Sea. Estuarine, Coastal and Shelf Science **115**, 33–39.

Gašparović B, Godrijan J, Frka S, *et al.* 2013. Adaptation of marine plankton to environmental stress by glycolipid accumulation. Marine Environmental Research **92**, 120–32.

Gašparović B, Kazazić SP, Cvitešić A, Penezić A, Frka S. 2015. Improved separation and analysis of glycolipids by Iatroscan thin-layer chromatography–flame ionization detection. Journal of Chromatography A **1409**, 259–67.

Gašparović B, Kazazić SP, Cvitešić A, Penezić A, Frka S. 2017. Corrigendum to 'Improved separation and analysis of glycolipids by Iatroscan

thin-layer chromatography–flame ionization detection' [J. Chromatogr. A 1409 (2015) 259–267. Journal of Chromatography A **1521**, 168–169.

Gaude N, Bréhélin C, Tischendorf G, Kessler F, Dörmann P. 2007. Nitrogen deficiency in Arabidopsis affects galactolipid composition and gene expression and results in accumulation of fatty acid phytyl esters. The Plant Journal **49**, 729–739.

Geider RJ. 1987. Light and temperature dependence of the carbon to chlorophyll *a* ratio in microalgae and cyanobacteria: implications for physiology and growth of phytoplankton. New Phytologist **106**, 1–34.

Gómez F. 2020. Symbioses of ciliates (Ciliophora) and diatoms (Bacillariophyceae): taxonomy and host–symbiont interactions. Oceans **1**, 133–155.

Guillard RRL. 1975. Culture of phytoplankton for feeding marine invertebrates. In: Smith WL, Chanley MH, eds. Culture of marine invertebrate animals: Proceedings – 1st Conference on Culture of Marine Invertebrate Animals, Greenport. Boston: Springer, 29–60.

Gustafsson B, Schenk F, Blenckner T, Eilola K, Meier H, Müller-Karulis B, Neumann T, Ruoho-Airola T, Savchuk O, Zorita E. 2012. Reconstructing the development of Baltic Sea eutrophication 1850–2006. Ambio **41**, 534–548.

Hamm C, Merkel R, Springer O, Jurkojc P, Maier C, Prechtel K, Smetacek V. 2003. Architecture and material properties of diatom shells provide effective mechanical protection. Nature **421**, 841–843.

Kim G, Seo K, Chen D. 2019. Climate change over the Mediterranean and current destruction of marine ecosystem. Scientific Reports **9**, 18813.

Intergovernmental Panel on Climate Change. 2021. Climate change 2021: the physical science basis. Geneva: Intergovernmental Panel on Climate Change.

International Organization for Standardization. 1992. ISO 10260:1992. Water quality — Measurement of biochemical parameters — Spectrometric determination of the chlorophyll-a concentration. Geneva: International Organization for Standardization.

Jiang Y, Yoshida T, Quigg A. 2012. Photosynthetic performance, lipid production and biomass composition in response to nitrogen limitation in marine microalgae. Plant physiology and biochemistry **54**, 70–77.

Ko E, Gorbunov MY, Jung J, Joo HM, Lee Y, Cho K, Yang EJ, Kang S, Park J. 2020. Effects of nitrogen limitation on phytoplankton physiology in the Western Arctic Ocean in summer. Journal of Geophysical Research: Oceans **125**, e2020JC016501.

Kobayashi K. 2016. Role of membrane glycerolipids in photosynthesis, thylakoid biogenesis and chloroplast development. Journal of Plant Research **129**, 565–580,

Lee J, Lee D, Kang J, Joo H, Lee JH, Lee H, Ahn SH, Lee S. 2017. The effects of different environmental factors on biochemical composition of particulate organic matters in Gwangyang Bay, South Korea. Biogeosciences **14**, 1903–1917.

Lee SD, Joo H, Lee J. 2014. Critical criteria for identification of the genus *Chaetoceros* (Bacillariophyta) based on setae ultrastructure. II. Subgenus *Hyalochaete*. Phycologia **53**, 614–638.

Lejeusne C, Chevaldonné P, Pergent-Martini C, Boudouresque CF, Pérez T. 2010. Climate change effects on a miniature ocean: the highly diverse, highly impacted Mediterranean Sea. Trends in Ecology and Evolution **25**, 250–60.

Liang Y, Koester JA, Liefer JD, Irwin AJ, Finkel ZV. 2019. Molecular mechanisms of temperature acclimation and adaptation in marine diatoms. The ISME Journal **13**, 2415–2425.

Lomas MW, Glibert PM. 2000. Comparisons of nitrate uptake, storage, and reduction in marine diatoms and flagellates. Journal of Phycology **36**, 903–913.

Longworth J, Wu D, Huete-Ortega M, Wright PC, Vaidyanathan S. 2016. Proteome response of *Phaeodactylum tricornutum*, during lipid accumulation induced by nitrogen depletion. Algal Research **18**, 213–224.

Lourenço SO, Barbarino E, Lavín PL, Lanfer Marquez UM, Aidar E. 2004. Distribution of intracellular nitrogen in marine microalgae: calculation of new nitrogen-to-protein conversion factors. European Journal of Phycology **39**, 17–32.

Lowry OH, Rosebrough NJ, Farr AL, Randall RJ. 1951. Protein measurement with the Folin phenol reagent. Journal of Biological Chemistry **193**, 265–275.

Ludwig W, Bouwman AF, Dumont F, Lespinas F. 2010. Water and nutrient fluxes from major Mediterranean and Black Sea rivers: past and future trends and their implications for the basin-scale budgets. Global Biogeochemical Cycles, **24**, GB0A13.

Malviya S, Scalco E, Audic S, *et al.* 2016. Insights into global diatom distribution and diversity in the world's ocean. Proceedings of the National Academy of Sciences, USA **113**, E1516– E1525.

Margalef R. 1978. Life-forms of phytoplankton as survival alternatives in an unstable environment. Oceanologica Acta **1**, 493–509.

Martin P, Van Mooy BAS, Heithoff A, Dyhrman ST. 2011. Phosphorus supply drives rapid turnover of membrane phospholipids in the diatom *Thalassiosira pseudonana*. The ISME Journal **5**, 1057–60.

Mathur S, Agrawal D, Jajoo A. 2014. Photosynthesis: response to high temperature stress. Journal of Photochemistry and Photobiology B **137**, 116–26.

Menden-Deuer S, Lessard EJ. 2000. Carbon to volume relationships for dinoflagellates, diatoms, and other protist plankton. Limnology and Oceanography **45**, 569–579.

Mizusawa N, Sakata S, Sakurai I, Sato N, Wada H. 2009. Involvement of digalactosyldiacylglycerol in cellular thermotolerance in *Synechocystis* sp. PCC 6803. Archives of Microbiology **191**, 595–601.

Mizusawa N, Sakata S, Sakurai I, Kubota H, Sato N, Wada H. 2013. Essential role of digalactosyldiacylglycerol for photosynthetic growth in *Synechocystis* sp. PCC 6803 under high-temperature stress. In: Photosynthesis research for food, fuel and the future. Advanced Topics in Science and Technology in China. Berlin, Heidelberg: Springer.

Murata N, Siegenthaler P. 1998. Lipids in photosynthesis: an overview. In: Siegenthaler P, Murata, N, eds. Lipids in photosynthesis: structure, function and genetics. Dordrecht: Kluwer Academic Publishers, 1–20.

Novak T, Godrijan J, Pfannkuchen DM, Djakovac T, Medić N, Ivančić I, Mlakar M, Gašparović B. 2019. Global warming and oligotrophication lead to increased lipid production in marine phytoplankton. Science of the Total Environment **668**, 171–183.

Novak T, Godrijan J, Pfannkuchen DM, Djakovac T, Mlakar M, Baricevic A, Tanković MS, Gašparović B. 2018. Enhanced dissolved lipid production as a response to the sea surface warming. Journal of Marine Systems **180**, 289–298.

Novosel N, Mišić Radić T, Zemla J, Lekka M, Čačković A, Kasum D, Legović T, Žutinić P, Gligora Udovič M, Ivošević DeNardis N. 2021. Temperature-induced response in algal cell surface properties and behavior. Journal of Applied Phycology **34**, 243–259.

Nykjaer L. 2009. Mediterranean Sea surface warming 1985–2006. Climate Research **39**, 11–17.

Palenik B, Kieber DJ, Morel FMM 1989. Dissolved organic nitrogen use by phytoplankton: The role of cell-surface enzymes. Biological Oceanography **6**, 347–354.

Parrish CC. 1988. Dissolved and particulate marine lipid classes: a review. Marine Chemistry **23**, 17–40.

Passow U, Carlson CA. 2012. The biological pump in a high CO_2 world. Marine Ecology Progress Series **470**, 249–271.

Penezić A, Gašparović B, Cuculić V, Strmečki S, Djakovac T, Mlakar M. 2022. Dissolved trace metals and organic matter distribution in the northern Adriatic, an increasingly oligotrophic shallow sea. Water **14**, 349.

Price CA. 1965. A membrane method for determination of total protein in dilute algal suspensions. Analytical Biochemistry **12**, 213–8.

Ras M, Steyer J, Bernard O. 2013. Temperature effect on microalgae: a crucial factor for outdoor production. Reviews in Environmental Science and Bio/Technology **12**, 153–164.

Rosset S, Koster G, Brandsma J, Hunt AN, Postle AD, D'Angelo C. 2019. Lipidome analysis of Symbiodiniaceae reveals possible mechanisms of heat stress tolerance in reef coral symbionts. Coral Reefs **38**, 1241–1253.

Sato N, Aoki M, Maru Y, Sonoike K, Minoda A, Tsuzuki M. 2003. Involvement of sulfoquinovosyl diacylglycerol in the structural integrity and heat-tolerance of photosystem II. Planta **217**, 245–51.

Sato N, Sonoike K, Tsuzuk M, Kawaguchi A. 1995. Impaired Photosystem II in a mutant of *Chlamydomonas reinhardtii* defective in sulfoquinovosyl diacylglycerol. European Journal of Biochemistry **234**, 16–23.

Sharma KK, Schuhmann H, Schenk PM. 2012. High lipid induction in microalgae for biodiesel production. Energies **5**, 1532–1553.

Sheehan C, Baker KG, Nielsen DA, Petrou K. 2020. Temperatures above thermal optimum reduce cell growth and silica production while increasing cell volume and protein content in the diatom *Thalassiosira pseudonana*. Hydrobiologia **847**, 4233–4248.

Slocombe SP, Ross M, Thomas N, McNeill S, Stanley MS. 2013. A rapid and general method for measurement of protein in micro-algal biomass. Bioresource Technology **129**, 51–7.

Smetacek VS. 1985. Role of sinking in diatom life-history cycles: ecological, evolutionary and geological significance. Marine Biology **84**, 239–251.

Smith REH, Gosselin M, Kattner G, Legendre L, Pesant S. 1997. Biosynthesis of macromolecular and lipid classes by phytoplankton in the Northeast Water Polynya. Marine Ecology Progress Series **147**, 231–242.

Smodlaka Tanković M, Baričević A, Ivančić I, Kužat N, Medić N, Pustijanac E, Novak T, Gašparović B, Marić Pfannkuchen D, Pfannkuchen MM. 2018. Insights into the life strategy of the common marine diatom *Chaetoceros peruvianus* Brightwell. PLoS One **13**, e0203634.

Strickland JDH, Parsons TR 1968. Determination of reactive phosphorus. In: A practical handbook of seawater analysis. Bulletin **167**. Ottawa: Fisheries Research Board of Canada, 49–56.

Sugimura Y, Suzuki Y. 1988. A high-temperature catalytic oxidation method for the determination of non-volatile dissolved organic carbon in seawater by direct injection of a liquid sample. Marine Chemistry **24**, 105–131.

Suzuki Y, Takahashi M. 1995. Growth responses of several diatom species isolated from various environments to temperature. Journal of Phycology **31**, 880–888.

Smil V. 2004. Enriching the Earth: Fritz Haber, Carl Bosch, and the transformation of world food production. Cambridge: MIT Press.

Uitz J, Claustre H, Gentili B, Stramski D. 2010. Phytoplankton class-specific primary production in the world's oceans: seasonal and interannual variability from satellite observations. Global Biogeochemical Cycles **24**, GB3016.

Vrana Špoljarić I, Novak T, Gašparović B, Kazazić SP, Čanković M, Ljubešić Z, Hrustić E, Mlakar M, Du J, Zhang R, Zhu Z. 2021. Impact of environmental conditions on phospholipid fatty acid composition: implications from two contrasting estuaries. Aquatic Ecology **55**, 1–20.